

Initial Design of Acoustic Vehicle Detector with Wind Noise Suppressor

Masato Uchino*, Sigemi Ishida*, Kazuo Kubo*, Shigeaki Tagashira†, Akira Fukuda*

*Graduate School/Faculty of Information Science and Electrical Engineering, Kyushu University, Japan

Email: {uchino, ishida, kubo, fukuda}@f.ait.kyushu-u.ac.jp

†Faculty of Informatics, Kansai University, Japan

Email: shige@res.kutc.kansai-u.ac.jp

Abstract—Vehicle detection is one of the fundamental tasks in the ITS (intelligent transport system). We are developing an acoustic vehicle detector that relies on two microphones at a sidewalk [1]. The vehicle detector successfully detected vehicles as well as their traveling directions. However, the detector has difficulties in vehicle detection in a high wind condition due to wind noise.

This paper presents a wind noise suppressor for the acoustic vehicle detector. Our simple idea is to remove frequency components corresponding to wind noise. Our acoustic vehicle detector relies on TDOA (time difference of arrival) of sound signals on two microphones to detect vehicles, which can be derived from a part of frequency components of vehicle sound signals. We experimentally analyze frequency components of wind noise and design a filter to reduce wind noise. Initial experimental evaluations reveal that our vehicle detector with a wind noise suppressor successfully detected vehicles with an F-measure of 0.77 in a normal wind condition.

Index Terms—ITS (intelligent transport system), vehicle detection, acoustic sensing, wind noise.

I. INTRODUCTION

The past decade has seen the rapid development of ITS (intelligent transport system). The main purpose of the ITS is to improve the safety, efficiency, dependability, and cost effectiveness of transportation systems. Route navigation with traffic information, collision avoidance, and connected vehicles are representative applications of the ITS.

In the ITS, vehicle sensing is one of the fundamental tasks. Vehicle sensors have installed on or above roads in some countries. The vehicle sensors, however, require roadwork closing target road sections for deployment and maintenance. The deployment of vehicle sensors is therefore limited to high traffic roads and highways in Japan. Some literature reported low-cost vehicle detector based on CCTVs [2, 3]. The CCTV approach is only applicable to high traffic roads. Current automatic vehicle sensing systems also suffer from a motorbike detection problem because of small coverage of vehicle sensors.

We are developing an acoustic vehicle detector that comes with low deployment and maintenance costs as another choice of low cost vehicle sensing for low traffic roads [1]. We use two microphones to capture acoustic signals generated from vehicle tires. We can detect vehicles on multiple lanes using low-cost microphones in a low height configuration from a sidewalk, which drastically reduces roadwork costs for deployment and maintenance. Our vehicle detector is capable

of detections of all vehicle types including motorbikes as long as vehicles generate sound.

We experimentally demonstrated that the acoustic vehicle detector successfully detected vehicles as well as their traveling direction. However, the detector fails to detect vehicles in a windy condition. The vehicle detector detects vehicles based on TDOA (time difference of arrival) of sound signals on two microphones. High wind causes wind noise on the two microphones, which damages TDOA estimation relying on a cross correlation function.

To tackle the wind problem, we present a wind noise suppressor for the acoustic vehicle detector. Our simple idea is to remove frequency components corresponding to wind noise. TDOA is estimated from a part of frequency components of vehicle sound signals. We therefore construct a filter that reduces wind noise frequency components prior to TDOA estimation. We don't limit the filter to use. In this paper, we design a noise suppression filter based on an experimental result. The experimental evaluations reveal that our wind noise suppressor effectively reduces the influence of wind noise, resulted in the vehicle detection with an F-measure of 0.77 in a normal wind condition.

Specifically, our key contributions are threefold:

- We present the design basics of a wind noise suppressor. We design a simple HPF (high pass filter), which effectively reduces influence of wind noise in vehicle detection.
- We experimentally show the frequency components of wind noise observed on four types of microphones.
- We experimentally show the vehicle detection performance of the vehicle detector with the wind noise suppressor.

The remainder of this paper is organized as follows. Section II describes acoustic vehicle detector and the influence of wind noise. Section III looks through related works on wind noise reduction. We present a wind noise suppressor in Section IV and Section V conducts experimental evaluations to demonstrate the effectiveness of the wind noise suppressor. Finally, Section VI concludes the paper.

II. ACOUSTIC VEHICLE DETECTOR

Figure 1 shows an overview of the acoustic vehicle detector presented in our previous work [1]. The vehicle detector

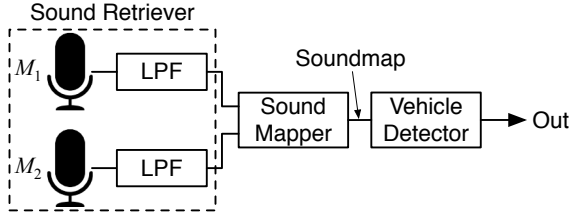


Fig. 1. Overview of acoustic vehicle detector

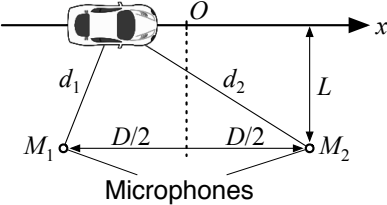


Fig. 2. Microphone setup

consists of a sound retriever, sound mapper, and vehicle detector.

The sound retriever consists of two microphones followed by LPFs (low pass filters). We install two microphones M_1 and M_2 separated by D at a road side distance L away from the road center as shown in Fig. 2 and derive vehicle sound signals. The sound signals are passed to a sound mapper after LPFs are applied to reduce high frequency environmental noise.

The sound mapper draws a sound map, which is a map of TDOA (time difference of arrival) of sound signals on the two microphones. The TDOA is estimated by finding a peak in a cross-correlation function $R(t)$ defined as

$$R(t) = \int s_1(t) s_2(t + r) dr, \quad (1)$$

where $s_1(t)$, $s_2(t)$ are sound signals on the two microphones. When the two microphones receive the same signals with time difference by Δt , i.e., $s_1(t) = s_2(t + \Delta t)$, the cross-correlation function $R(t)$ becomes maximum at $t = \Delta t$. In our implementation, we use a GCC (generalized cross-correlation) function [4], which is commonly used in a field of acoustic source localization. Sound map points correspond to GCC peak at a specific time window.

Figure 3 shows a typical example of sound map. Passing vehicles are moving from left to right or right to left in front of the microphones, resulting in S-curves on a sound map. The S-curve is given by an equation below:

$$\Delta t = \frac{1}{c} \left\{ \sqrt{\left(vt + \frac{D}{2}\right)^2 + L^2} - \sqrt{\left(vt - \frac{D}{2}\right)^2 + L^2} \right\}, \quad (2)$$

where v denote the speed of a vehicle and c denote the speed of sound in air. The direction of an S-curve depends on traveling directions of vehicles. In this example, four vehicles were passing: one from left to right and three from right to left.

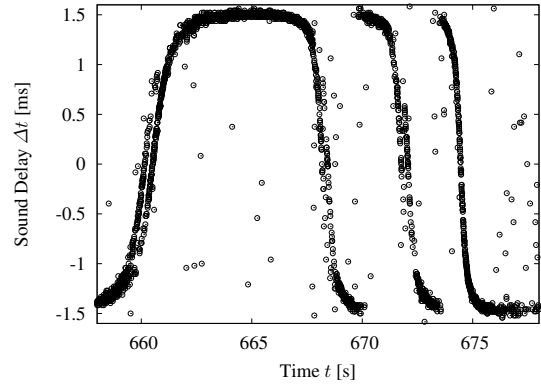


Fig. 3. Typical example of sound map

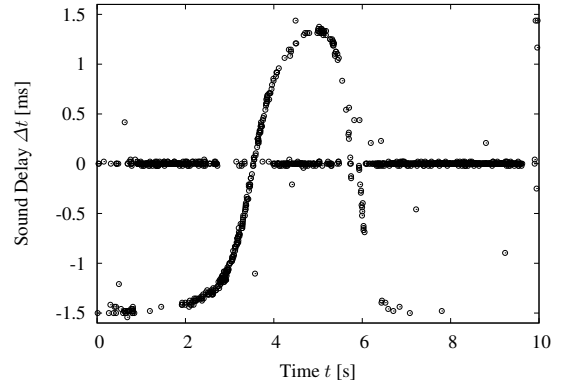


Fig. 4. Sound map example in windy condition

The vehicle detector finally detects S-curves on a sound map using a RANSAC (random sample consensus) robust estimation method [5]. The RANSAC fits the sound map model given in Eq. (2) to sound map points. The RANSAC always gives an estimated S-curve that best fits to sound map points even if no vehicle is passing. We apply a simple filter to detect vehicle passing. For detections of successive and simultaneous passing vehicles, we remove sound map points corresponding to the detected vehicles.

The acoustic vehicle detector highly fails to detect vehicles in a windy condition. In a windy condition, wind noise generates invalid cross-correlation peaks resulting in noisy sound map. The two microphones receive wind noise, which are independent because the wind noise is generated on each microphone. The two microphones also receive the same sound signals from an identical jig holding the microphones. The sound signals generated on the same jig reach at the two microphones with small time difference, which results in noise points around $\Delta t = 0$ on a sound map.

Figure 4 shows an example of sound map in a windy condition. When no vehicle was passing, many noise points around $\Delta t = 0$ appeared on a sound map because of small correlation of wind noise. Even when a vehicle was passing, sound map points around $\Delta t = 0$ sometimes appeared in a windy condition.

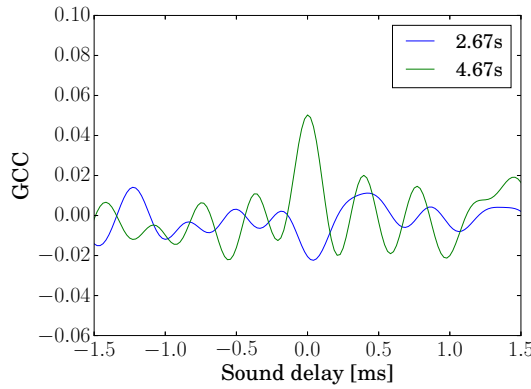


Fig. 5. GCC (generalized cross-correlation) result in windy condition

Figure 5 shows an example of GCC result at time $t = 2.67, 4.67$ s in Fig. 4. At $t = 2.67$, 4.67 s, sound delays were $\Delta t = -1.23, 1.46$ ms, respectively. At $t = 2.67$ s, we can see a peak at $\Delta t = -1.23$ ms in Fig. 5. However, at $t = 4.67$ s, we can see a GCC peak at $\Delta t = 0$ ms, which is different from the correct sound delay of $\Delta t = -1.46$ ms.

III. RELATED WORKS

To the best of knowledge, this paper is a first trial tackling the wind noise problem in the field of acoustic vehicle sensing. In this section, we briefly look through noise reduction methods and techniques for acoustic sensors.

A. Noise Reduction Method

Moragues et al. proposed a noise reduction method using a microphone array [6]. This method reduces noise by combining SRP-PHAT (steered-response power phase transform) and GCC (generalized cross correlation), which are sound source localization methods. This method, however, highly fails to reduce unsteady noise such as wind noise. Moreover, this method is only applicable to sound signals derived on omnidirectional microphones.

For unsteady noise reduction, EMD (empirical mode decomposition) based approach have been reported [7, 8]. Sound signals are decomposed into different frequency components using EMD, which are more divided into signals and noises based on an IMF (intrinsic mode function) of the each frequency components. The EMD-based approach effectively reduces noise, though the approach requires more than three microphones.

B. Wind Noise Reduction Technique

Windshield is a intuitive approach to reduce wind noise. JIS C1400-11 is defined by JIS (Japanese industrial standards), which is a microphone setup robust to wind noise. Microphones are covered with two windshields to reduce the influence of wind, which is effective for wind noise generated by microphones themselves. However, this approach requires two large windshields, which puts restriction on deployment

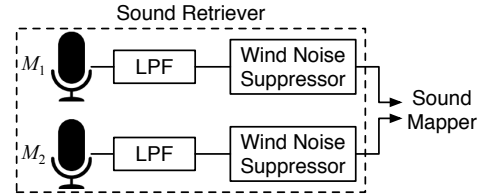


Fig. 6. Overview of sound retriever with wind noise suppressor

on a sidewalk. Moreover, the windshields have a limited tolerance to high frequency air-flow noise.

Wind jammers are popular approach for wind noise reduction. Wind jammers are available at a low cost and reduce the energy suppressing wind noise. Our approach can be combined with this wind jammer approach to enhance a tolerance to wind noise.

IV. ACOUSTIC VEHICLE DETECTION WITH WIND NOISE SUPPRESSOR

A. Approach

Our simple idea is to remove wind noise frequency components prior to TDOA estimation. The acoustic vehicle detector presented in Section II relies on TDOA of vehicle sound signals, which composed of many frequency components. We remove noise frequency components while avoiding vehicle sound components. We develop a filter that reduces wind noise frequency components other than the vehicle sound components.

Figure 6 shows an overview of a sound retriever with a wind noise suppressor in a vehicle detector. Compared to a sound retriever in Fig. 1, we add blocks named *wind noise suppressor*, which are actually a filter reducing wind noise frequency components. The following subsections give design details of the wind noise suppressor.

B. Wind Noise Suppressor

Wind noise suppressor is actually a filter reducing wind noise components other than vehicle sound components. In the filter design, we avoid to drop vehicle sound frequency components. Majority of frequency components of sound signals generated by vehicle tires are from 1 kHz to 2 kHz [9]. For reference, we tried to detect vehicles using the frequency components from 1 kHz and 2 kHz. We added BPFs (band pass filters) in the sound retriever and drew a sound map to get S-curves, which the RANSAC algorithm successfully detected. We therefore avoid to remove the frequency components from 1 kHz to 2 kHz when designing a filter for wind noise suppressor.

We don't limit the actual design of the filter including filter types. We can employ general noise reduction method mainly proposed in the fields of image and audio signal processing. Typical examples of noise reduction methods are Wavelet, principal component analysis, SVD (singular value decomposition), or EMD [7, 8, 10–14].

In this paper, we use a simple HPF (high pass filter) designed based on preliminary experiment, as presented in the following subsection.

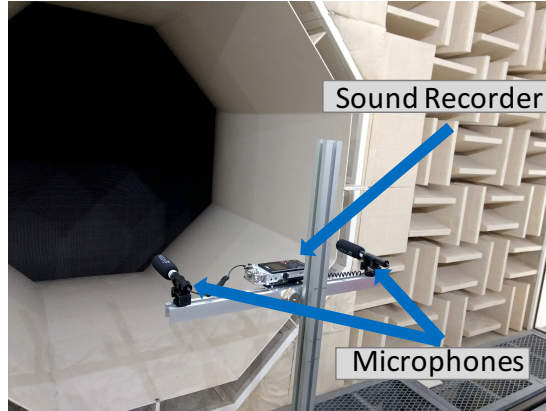


Fig. 7. Experiment setup in wind tunnel

TABLE I
MICROPHONE MODELS USED IN DESIGN EXPERIMENT OF WIND NOISE SUPPRESSOR

Microphone model	Vendor
SGM-990	AZDEN
AT9942	Audio Technica
AT9944	Audio Technica
ECM-CG60	Sony

C. Experimental Design of Wind Noise Suppressor

In this subsection, we design a HPF to reduce wind noise frequency components while preserving vehicle sound components based on experiment. We determine a cut-off frequency of the HPF based on an experiment conducted in a wind tunnel.

Figure 7 shows experiment setup in an atmospheric wind tunnel. We installed two microphones in a wind path at a height of 1.5 meters from the ground. The two microphones were separated by 50 centimeters. We recorded wind noise at a sampling rate of 48 kHz with 16-bit word length using a Sony PCM-D100 sound recorder. Wind speed was changed from 1.0 m/s to 15.0 m/s at a 1.0-m/s step.

We used four microphone models to measure wind noise because wind noise is dependent on microphone models. Microphone models used in the experiment are shown in Table I. We recorded wind noise with each microphone model at each wind speed. Then we analyzed frequency components of the wind noise.

Figure 8 shows frequency components of wind noise, which is an example derived by AZDEN SGM-990 microphones. Although frequency components of wind noise are dependent on microphone models and wind speed, we found that majority of wind noise components were less than 500 Hz. Based on this result, we designed a HPF with a cut-off frequency of 500 Hz as a wind noise suppressor in this paper.

Figure 9 shows an example sound map derived after the wind noise suppressor was applied, which shows the same time section as Fig. 4. Comparing Figures 4 with 9, the wind noise suppressor reduces sound map points around $\Delta t = 0$, resulting in a more clear S-curve. The wind noise suppressor

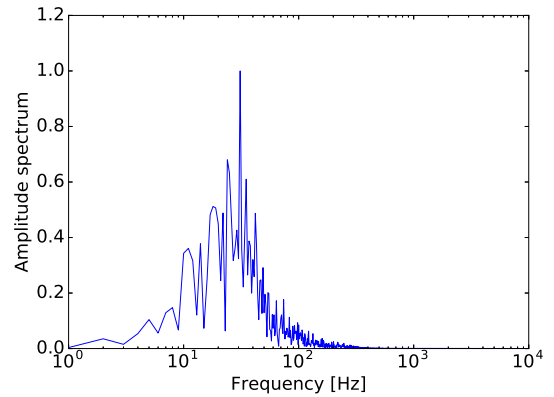


Fig. 8. Wind noise spectrum measured by AZDEN SGM-990 microphones at wind speed of 8.0 m/s

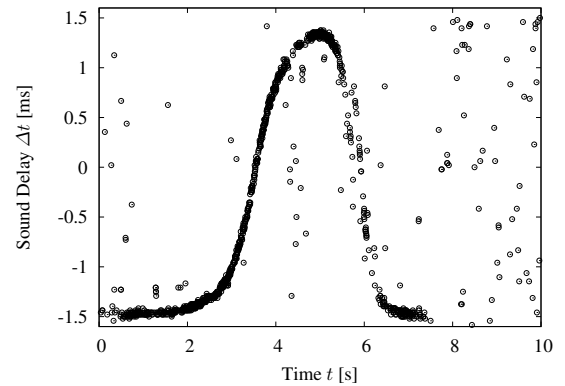


Fig. 9. Sound map example with wind noise suppressor

reduces wind noise and a GCC peak is emphasized in TDOA estimation.

Figure 10 shows an example GCC derived after the wind noise suppressor was applied, which show the same time section as Fig. 5. Comparing Figures 5 with 10, GCC peaks correctly appear after applying wind noise suppressor at $\Delta t = -1.23, 1.46$ ms for $t = 2.67, 4.67$ s, respectively.

V. EVALUATION

As an initial evaluation, we conducted experiments to evaluate detection performance of our vehicle detector with the wind noise suppressor.

A. Experiment Setup

Figure 11 shows an experiment setup. A target road in our university campus has two lanes, one lane in each direction. Two microphones were installed approximately two meters away from the road center. Referring to our previous paper [15], we set distance between the two microphones to 50 centimeters. The height of the detector from the ground was 1 meter. We recorded vehicle sound for approximately 20 minutes using a Sony PCM-D100 sound recorder with AZDEN SGM-990 microphones. The sound was recorded at a sampling rate of 48 kHz and with word length of 16 bits.

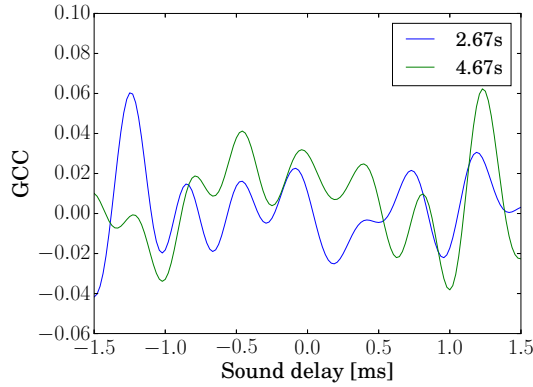


Fig. 10. GCC example with wind noise suppressor

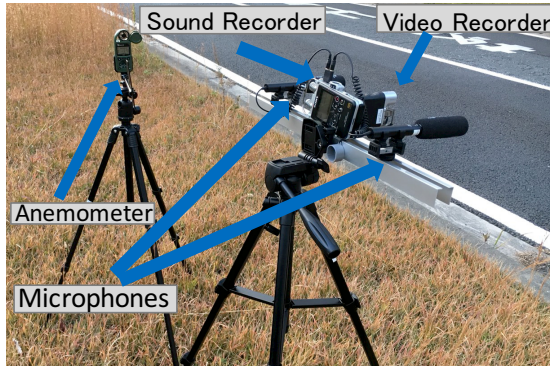


Fig. 11. Experiment setup

We also recorded video monitoring the road as ground truth data. During the experiment, 133 vehicles passed. As for wind measurement, we recorded wind speed by installing an Kestrel5500 anemometer. Average and maximum wind speed during our experiment were 5.2 m/s and 8.6 m/s, respectively.

B. Detection Performance in Normal Wind Condition

We first evaluated detection performance in a normal wind condition. We evaluated the numbers of true positives (TPs), false negatives (FNs), and false positives (FPs). TPs, FNs, and FPs are defined as the cases that a vehicle is detected when a vehicle is passing, that no vehicle is detected when a vehicle is passing, and that a vehicle is detected when no vehicle is passing, respectively.

We also calculated precision, recall, and F-measure defined as:

$$\text{Precision} = \frac{\text{TP}}{\text{TP} + \text{FP}}, \quad (3)$$

$$\text{Recall} = \frac{\text{TP}}{\text{TP} + \text{FN}}, \quad (4)$$

$$\text{F}_{\text{measure}} = \frac{2 \cdot \text{Precision} \cdot \text{Recall}}{\text{Precision} + \text{Recall}}. \quad (5)$$

Table II shows detection performance, i.e., the numbers of TPs, FNs, and FPs as well as calculated precision, recall, and F-measure. Table II indicates the following:

TABLE II
VEHICLE DETECTION PERFORMANCE

(a) with wind noise suppressor			
	Left to Right	Right to Left	Total
TPs	69	37	106
FNs	15	12	27
FPs	27	8	35
Precision	0.72	0.82	0.75
Recall	0.82	0.76	0.80
F-measure	0.77	0.79	0.77

(b) without wind noise suppressor			
	Left to Right	Right to Left	Total
TPs	67	37	104
FNs	17	12	29
FPs	49	23	72
Precision	0.58	0.62	0.59
Recall	0.80	0.76	0.78
F-measure	0.67	0.68	0.67

TABLE III
VEHICLE DETECTION PERFORMANCE OF THE VEHICLE DETECTOR WITH WIND NOISE SUPPRESSOR IN HIGH WIND CONDITION

	Left to Right	Right to Left	Total
TPs	22	17	39
FNs	66	8	74
FPs	31	16	47
Precision	0.42	0.52	0.45
Recall	0.22	0.68	0.35
F-measure	0.31	0.59	0.39

- The vehicle detection system with the wind noise suppressor showed the detection performance with an F-measure of 0.77. Compared to the vehicle count system without the wind noise suppressor, F-measure was increased by 10 points.
- Precision was significantly improved by our wind noise suppressor. The wind noise suppressor effectively reduced the numbers of FP detections, resulted in the increase in the precision.
- Recall of the vehicle detector with and without the wind noise suppressor was almost the same. FNs were mainly caused by simultaneous and sequential passing vehicles, which cannot be addressed by the wind noise suppressor.

The above results confirm that the vehicle detector with the wind noise suppressor successfully detected vehicles with an F-measure greater than the detector without wind noise suppressor.

C. Detection Performance in High Wind Condition

As a further evaluation of our vehicle detector, we evaluated the detection performance in a high wind condition. We used the same experiment setup as the evaluation in a normal wind condition presented in the previous subsection. The vehicle sound was recorded for approximately 12 minutes, in which 113 vehicles passed. Average and maximum wind speed in the experiment were 6.6 m/s and 13.3 m/s, respectively.

Comparing Tables II and III, we can see that precision and recall were significantly decreased by high wind. The decrease was caused by noise points on a sound map. As described in Section II, wind noise generates noise points around $\Delta t = 0$

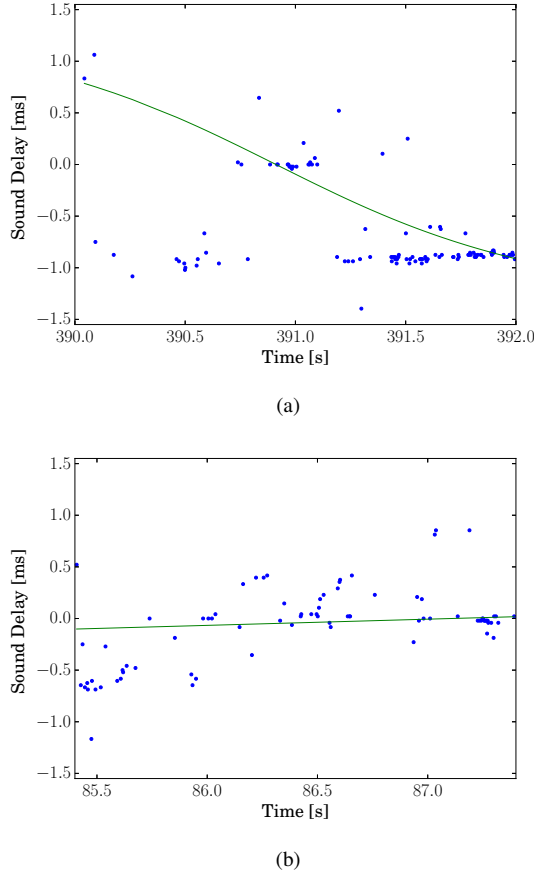


Fig. 12. (a) False positive (FP) and (b) false negative (FN) detections in a high wind condition

on a sound map. Wind noise suppressor failed to completely remove the noise points in a high wind condition. The vehicle detector mistakenly detected vehicles between a tail of an S-curve and a noise point, which resulted in FPs. FNs also happened when there were too many noise points resulting in a sparse S-curve on a sound map.

Figure 12 shows examples of FP and FN detections in a high wind condition. As shown in Fig. 12a, an invalid S-curve between a tail of a bold S-curve and noise points around $\Delta t = 0$ was estimated by the RANSAC algorithm, resulted in a FP detection. Figure 12b shows an example of FN detection. Two S-curves drawn by a bus were ignored, resulting in FN. Further investigation on detection algorithm is required to improve detection performance.

VI. CONCLUSION

In this paper, we presented an acoustic vehicle detector with a wind noise suppressor to improve robustness to wind noise. Our simple idea is to remove wind noise frequency components other than vehicle sound components prior to vehicle detection. We implemented the acoustic vehicle detector with the noise suppressor and conducted initial experimental

evaluations. The initial experiments revealed that our vehicle detector with the wind noise suppressor successfully detected vehicles with an F-measure of 0.77 in a normal wind condition, although an F-measure in a high wind condition decreased down to 0.39. The wind noise suppressor has limited contribution to the robustness to wind noise in a high wind condition. We work on this high-wind problem as our future work.

ACKNOWLEDGMENT

This work was supported in part by JSPS KAKENHI Grant Numbers JP15H05708, JP17K19983, JP17H01741 and JP18K18041 as well as the Cooperative Research Project of the Research Institute of Electrical Communication, Tohoku University.

REFERENCES

- [1] S. Ishida, J. Kajimura, M. Uchino *et al.*, “SAVeD: Acoustic vehicle detector with speed estimation capable of sequential vehicle detection,” in *Proc. IEEE Conf. Intelligent Transportation Systems (ITSC)*, Nov. 2018, pp. 906–912.
- [2] N. Buch, M. Cracknell, J. Orwell *et al.*, “Vehicle localisation and classification in urban CCTV streams,” in *Proc. ITS World Congress*, Sep. 2009, pp. 1–8.
- [3] A. Nurhadiyatna, B. Hardjono, A. Wibisono *et al.*, “ITS information source: Vehicle speed measurement using camera as sensor,” in *Proc. Int. Conf. on Advanced Computer Science and Information Systems (ICACSIS)*, Dec. 2012, pp. 179–184.
- [4] C. H. Knapp and G. C. Carter, “The generalized correlation method for estimation of time delay,” *IEEE Trans. Acoust., Speech, Signal Process.*, vol. 24, no. 4, pp. 320–327, Aug. 1976.
- [5] M. A. Fischler and R. C. Bolles, “Random sample consensus: A paradigm for model fitting with applications to image analysis and automated cartography,” *Commun. ACM*, vol. 24, no. 6, pp. 381–395, Jun. 1981.
- [6] J. Moragues, L. Vergara, J. Gosálbez *et al.*, “Background noise suppression for acoustic localization by means of an adaptive energy detection approach,” in *Proc. IEEE Int. Conf. on Acoustics, Speech, and Signal Processing (ICASSP)*, Mar.–Apr. 2008, pp. 2421–2424.
- [7] L. Xiaofeng and L. Mingjie, “The de-noising method for EMD threshold based on correlation,” in *Proc. IEEE Int. Conf. Signal Processing (ICSP)*, Oct. 2010, pp. 2613–2616.
- [8] Y. Kopsinis and S. McLaughlin, “Development of EMD-based denoising methods inspired by Wavelet thresholding,” *IEEE Trans. Signal Process.*, vol. 57, no. 4, pp. 1351–1362, Apr. 2009.
- [9] H. Wu, M. Siegel, and P. Khosla, “Vehicle sound signature recognition by frequency vector principal component analysis,” in *Proc. IEEE Instrumentation and Measurement Technology Conf. (IMTC)*, vol. 1, May 1998, pp. 429–434.
- [10] M. Aminghafari, N. Cheze, and J.-M. Poggi, “Multivariate denoising using Wavelets and principal component analysis,” *Computational Statistics & Data Analysis*, vol. 50, no. 9, pp. 2381–2398, May 2006.
- [11] G. Chen and S.-E. Qian, “Denoising of hyperspectral imagery using principal component analysis and Wavelet shrinkage,” *IEEE Trans. Geosci. Remote Sens.*, vol. 49, no. 3, pp. 973–980, Mar. 2011.
- [12] L. Du, B. Wang, P. Wang *et al.*, “Noise reduction method based on principal component analysis with beta process for micro-doppler radar signatures,” *IEEE J. Sel. Topics Appl. Earth Observ. Remote Sens.*, vol. 8, no. 8, pp. 4028–4040, Aug. 2015.
- [13] K. Shin, J. K. Hammond, and P. R. White, “Iterative SVD method for noise reduction of low-dimensional chaotic time series,” *Mechanical Systems and Signal Processing*, vol. 13, no. 1, pp. 115–124, Jan. 1999.
- [14] Q. Guo, C. Zhang, Y. Zhang *et al.*, “An efficient SVD-based method for image denoising,” *IEEE Trans. Circuits Syst. Video Technol.*, vol. 26, no. 5, pp. 868–880, May 2016.
- [15] S. Ishida, K. Mimura, S. Liu *et al.*, “Design of simple vehicle counter using sidewalk microphones,” in *Proc. ITS EU Congress*, EU-TP0042, Jun. 2016, pp. 1–10.